Hopcroft, P. O., & Valdes, P. J. (2015). How well do last glacial maximum tropical temperatures constrain equilibrium climate sensitivity?. Geophysical Research Letters, 42(13), 5533-5539. 10.1002/2015GL064903

AGU PUBLICATIONS

Geophysical Research Letters

RESEARCH LETTER
10.1002/2015GL064903

How well do simulated last glacial maximum tropical temperatures constrain equilibrium climate sensitivity?

Peter O. Hopcroft[1] and Paul J. Valdes[1]

[1] Bristol Research Initiative for the Dynamic Global Environment, School of Geographical Sciences, University of Bristol, Bristol, UK

Key Points:
- New LGM simulations show no tropical temperature to climate sensitivity relation
- This is caused by a model complexity, especially due to Earth System components
- It is unclear how inferred ECS will change as more model components are included

Supporting Information:
- Texts S1 and S2, Figures S1–S4, and Tables S1–S3

Correspondence to:
P. O. Hopcroft,
peter.hopcroft@bristol.ac.uk

Citation:
Hopcroft, P. O., and P. J. Valdes (2015), How well do simulated last glacial maximum tropical temperatures constrain equilibrium climate sensitivity?, *Geophys. Res. Lett.*, *42*, 5533–5539, doi:10.1002/2015GL064903.

Received 11 JUN 2015
Accepted 13 JUN 2015
Accepted article online 18 JUN 2015
Published online 14 JUL 2015

Abstract Previous work demonstrated a significant correlation between tropical surface air temperature and equilibrium climate sensitivity (ECS) in PMIP (Paleoclimate Modelling Intercomparison Project) phase 2 model simulations of the last glacial maximum (LGM). This implies that reconstructed LGM cooling in this region could provide information about the climate system ECS value. We analyze results from new simulations of the LGM performed as part of Coupled Model Intercomparison Project (CMIP5) and PMIP phase 3. These results show no consistent relationship between the LGM tropical cooling and ECS. A radiative forcing and feedback analysis shows that a number of factors are responsible for this decoupling, some of which are related to vegetation and aerosol feedbacks. While several of the processes identified are LGM specific and do not impact on elevated CO_2 simulations, this analysis demonstrates one area where the newer CMIP5 models behave in a qualitatively different manner compared with the older ensemble. The results imply that so-called Earth System components such as vegetation and aerosols can have a significant impact on the climate response in LGM simulations, and this should be taken into account in future analyses.

1. Introduction

The last glacial maximum (LGM) is defined as the period during the last glacial-interglacial cycle when ice sheet volume was at a maximum [e.g., *Mix et al.*, 2001], from 23 to 19 kyr B.P. (before present). This period has been a focus of paleoclimate study for several decades, because it constitutes an example of a near-equilibrium global climate state which is very different from today's. Several global synthesis of paleo-environmental reconstructions have been produced [e.g., *Kohfeld and Harrison*, 2001; *Prentice et al.*, 2000; *MARGO Project Members*, 2009; *Bartlein et al.*, 2011], and these allow coupled climate model simulations of this time period to be evaluated in detail [e.g., *Harrison et al.*, 2013].

The climate of the LGM is characterized by large ice sheets which dominated the Northern Hemisphere (e.g., as reconstructed by *Peltier* [2004]) and by a significant reduction in the concentration of the natural greenhouse gases (GHG) compared to the preindustrial [*Petit et al.*, 1999; *Spahni et al.*, 2005]. The astronomical configuration was also different, but this had a minor climatic forcing seasonally or in the annual mean [*Berger and Loutre*, 1991]. The radiative forcing from these ice sheets and reduced GHG levels is estimated to be approximately equal in magnitude to that from a quadrupling of CO_2, thus making the LGM one candidate time period for studying well-resolved large-scale change in the global environment [*Braconnot et al.*, 2012].

A number of studies have aimed to quantify how well the LGM climate might be able to constrain the value of equilibrium climate sensitivity (ECS). *Crucifix* [2006] demonstrated using four coupled general circulation models (GCMs) from phase 2 of PMIP (Paleoclimate Modelling Intercomparison Project) that there was no clear relationship between climatic feedbacks operating at the LGM and in response to increased CO_2 at the global scale. This was shown to derive from multiple factors including (i) LGM specific forcings (namely, ice sheets) and feedbacks such as a marked cloud feedback response to the ice sheets in the Northern Hemisphere and (ii) differential responses in some models (particularly MIROC3.2) in cloud feedbacks in warmer versus cooler climates.

Using MIROC3.2, *Yoshimori et al.* [2009] analyzed some of these issues in more detail by decomposing the climatic feedbacks operating in response to increased and decreased atmospheric CO_2 and in response to LGM boundary conditions (which include reduced GHG levels). They found differences in the cloud feedback

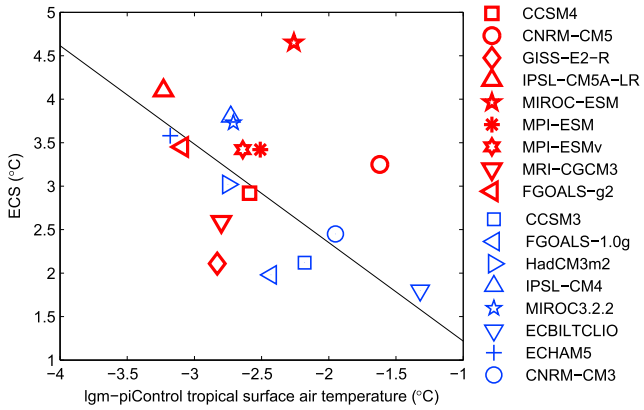

Figure 1. The relationship between ECS and tropical lgm-piControl temperature anomalies (ΔT_{trop}) for PMIP2 and CMIP5-PMIP3 ensembles of LGM and preindustrial simulations. The correlation for eight PMIP2 models is −0.8 and is +0.1 for nine PMIP3 simulations. The linear regression of the PMIP2 models is shown by the black line.

operating in response to warmer versus colder climates which are thought to derive from a simulated displacement of mixed-phase clouds in the model. The results of *Crucifix* [2006] suggest that this process is not operating equally in all models however.

Following this prior work, *Hargreaves et al.* [2012] restricted the analysis to the tropics. Using an expanded ensemble of seven PMIP2 models, they showed a statistically significant relationship between model ECS and simulated LGM tropical cooling. This is likely because the dominant driver of tropical temperature change is GHG forcing in these LGM simulations. *Hargreaves et al.* [2012] postulated that combining reconstructions of LGM tropical temperatures and model results could provide constraints on the real climate system ECS value.

The LGM simulation is now a core part of the Coupled Model Intercomparison Project (CMIP) phase 5 meaning that many models used to project future changes or to perform idealized perturbation experiments are also evaluated under paleoclimate boundary conditions. The models used in CMIP5 also differ markedly from those used in CMIP3 and PMIP2. In addition to increases in the level of complexity in various process representations, many of the models now include Earth System components such as dynamic vegetation or interactive aerosols. We therefore expand the analysis of *Hargreaves et al.* [2012] to include results from nine model simulations of the LGM from CMIP5-PMIP3. This follows a similar analysis in *Schmidt et al.* [2014] (also shown in the IPCC AR5) which showed that the relationship between ECS and LGM temperature anomalies was less robust in the CMIP5 models than in the PMIP2 simulations. Here we address this issue directly by analyzing the radiation budget in each simulation and comparing with the results from idealized abrupt4×CO_2 simulations.

2. Methods

CMIP5 data were obtained for piControl, lgm, and abrupt4×CO_2 experiments. The latter were averaged over years 101–150. A list of models analyzed with their calculated equilibrium climate sensitivities is given in Table S1 in the supporting information. We derive equilibrium climate sensitivities for the CMIP5 models using the method of *Gregory et al.* [2004] and use values for the PMIP2 models from *Forster and Taylor* [2006] which are also calculated using this method. These values are given in Table S1 and are shown in Figure 1.

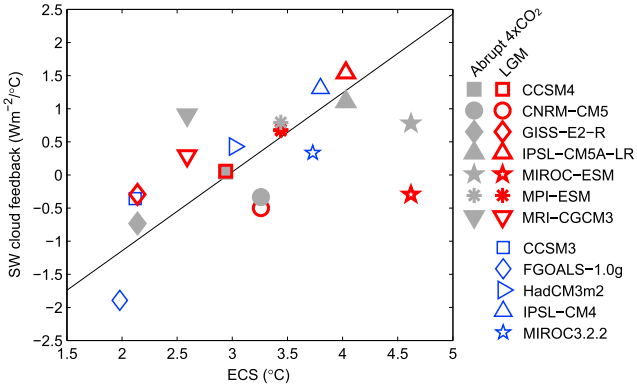

Figure 2. Short-wave cloud radiative feedbacks in PMIP2, PMIP3, and abrupt4×CO_2 simulations. The SW cloud feedback is calculated using the approximate partial radiative perturbation method [*Taylor et al.*, 2007] and is normalized by the simulated surface temperature change averaged over the same region. The linear regression of the PMIP2 models is shown by the black line.

The short-wave (SW) radiative forcing and feedbacks in each model are decomposed using the APRP method of *Taylor et al.* [2007]. This has been used in many previous studies [e.g., *Crucifix*, 2006; *Braconnot et al.*, 2012; *Brady et al.*, 2013; *Hopcroft and Valdes*, 2014]. Essentially at a grid box level for each model, monthly mean total cloud cover and radiation diagnostics for the surface and

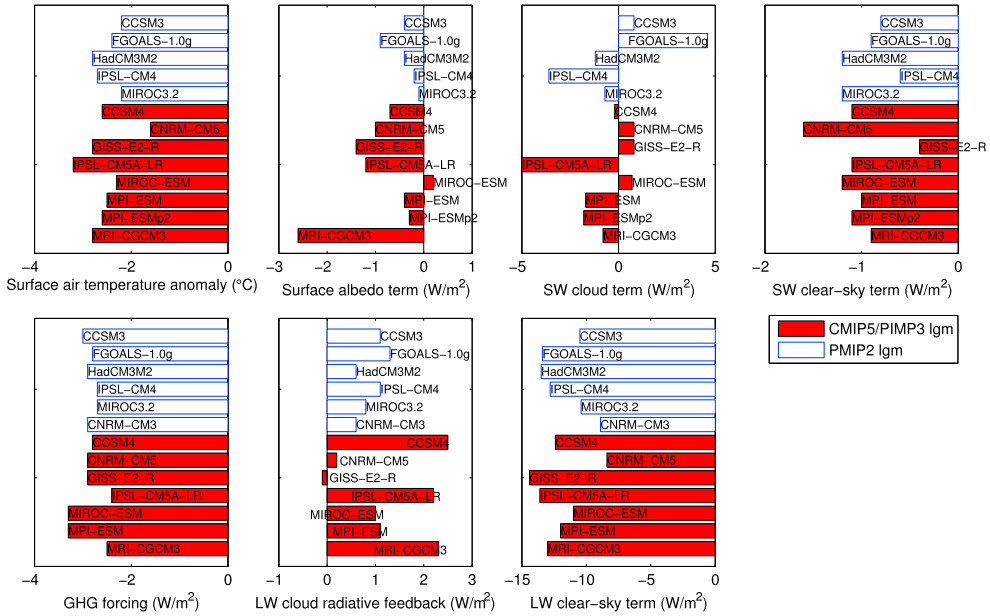

Figure 3. Tropical regional averages of surface temperature anomalies and short-wave (SW) and long-wave (LW) radiative feedbacks in PMIP2 and PMIP3 LGM simulations compared to the respective preindustrial control simulations. SW terms are calculated using APRP method [*Taylor et al.*, 2007], while the LW terms are calculated as described in the text. The LW cloud term is calculated as the difference between TOA all-sky and clear-sky fluxes.

top of the atmosphere (TOA) for all-sky and clear-sky conditions are used in a simplified representation of the surface and atmospheric properties to calculate the contributions from the land surface albedo, clouds, and clear-sky atmospheric absorption and scattering to the short-wave forcing and feedbacks operating in the model. These values are summarized for the PMIP2 and PMIP3 models in Figure 2 which shows short-wave cloud feedbacks and Figure 3, for other fields. Both figures show averages over the tropics, the focus of this work. A similar analysis of the abrupt4×CO_2 simulations is shown in the supporting information.

The long-wave (LW) fluxes are also shown in Figure 3 for the LGM (see the supporting information for the abrupt4×CO_2 simulations). The greenhouse gas forcing is calculated from the 2×CO_2 (for PMIP2 models) or 4×CO_2 (for CMIP5 models) greenhouse gas forcing, scaled to the LGM GHG change following *Crucifix* [2006]. The figure also shows the TOA LW cloud radiative forcing diagnosed as the difference between the all-sky and clear-sky LW fluxes at the top of the atmosphere. The estimated GHG feedback term is also shown. This latter term is derived from the difference between the TOA and surface clear-sky outgoing LW radiation and is corrected for the Planck response to the LGM orographic change using a uniform atmospheric lapse rate of 6.5 K km^{-1}.

3. Results

Figure 1 shows ECS for the PMIP2 and PMIP3 models as a function of their simulated lgm-piControl temperature change averaged over the tropics and here denoted ΔT_{trop}. This shows a strong correlation for PMIP2 models (further supported here by the inclusion of CNRM-CM3 values). The PMIP2 ECS values are slightly different from those used by *Hargreaves et al.* [2012], which were based on slab ocean runs. The PMIP2 ECS values derived from the Gregory analysis strengthens the negative correlation between climate sensitivity and the lgm-piControl tropical temperature change for each model, changing from −0.75 to −0.79. However, the same analysis conducted for PMIP3 models shows that this relationship does not hold. The correlation is close to zero, with PMIP3 models showing similar levels of cooling at the LGM but with a wide range of ECS values. A similar analysis for the abrupt4×CO_2 simulations with these same models conducted as part of CMIP5 shows a strong relationship between ECS and tropical warming, and this is shown in the supporting information Figure S1. Thus, the question arises as to why this relationship appears to apply in the PMIP2 (CMIP3) LGM models but not in the newer CMIP5 ensemble.

Five of the PMIP3 models fall close to the PMIP2 relationship between ECS and ΔT_{trop}. These models are CCSM4, FGOALS-g2, IPSL-CM5A-LR, MPI-ESM, and MRI-CGCM3. Of the remaining three models, two have relatively high ECS values but show small changes in tropical temperatures: MIROC-ESM (ECS = 4.65) and CNRM-CM5 (ECS = 3.25), while GISS-E2-R has a relatively low ECS value but shows a larger change in ΔT_{trop}. The three models which behave least like the PMIP2 ensemble form the bulk of the analysis below.

A comparison of the spatial correlation of ECS against surface temperature following *Hargreaves et al.* [2012] (Figure S2) demonstrates that the relationship between ECS and temperature anomalies is only weakly evident in the North Atlantic in PMIP3, while in the PMIP2 models it is evident across much of the tropics (as shown before). Additionally, the relationship is shown to hold for the four models in PMIP2 for which full radiation diagnostics are available.

Since the SW feedbacks from clouds are known to play a pivotal role in the intermodel spread in climate sensitivity [e.g., *Dufresne and Bony*, 2008] this is analyzed first. Figure 2 shows SW cloud radiative feedback as a function of climate sensitivity. The SW cloud terms are divided by the simulated tropical temperature change in this comparison. The feedback strength increases across most models as a function of ECS consistently across the two different experiments. MIROC-ESM and MRI-CGCM3 show the largest exceptions with clear differences between the warmer and cooler scenarios. MIROC-ESM shows relatively weak SW cloud effect given its high climate sensitivity. The discrepancy is much larger for the lgm simulation compared to the abrupt4×CO_2 simulation, a point we return to below. MRI-CGCM3 behaves in the opposite sense and shows a stronger cloud feedback than would be expected from its ECS value (given the behavior of the other models). In this case the LGM simulation also shows a weaker cloud SW feedback than the abrupt4×CO_2 simulation. The majority of the other models, however, show a reasonable agreement in terms of the strength of the cloud feedback, demonstrating symmetry in cooler versus warmer climate states. Apart from MIROC-ESM and MRI-CGCM3, this suggests that decoupling between the tropical temperature change and ECS in PMIP3 is related to processes other than SW radiative effects of clouds.

The remaining short-wave radiation budget terms are compared in Figure 3. There is great variability in the SW cloud term across both the PMIP2 and PMIP3/CMIP5 lgm ensembles. In contrast the SW surface albedo term is much more variable in the newer PMIP3/CMIP5 ensemble. The largest value found in MRI-CGCM3 is caused by prescribing bare soil areas over new land areas for the LGM in this model (K. Yoshida, personal communication, 2014). The clear-sky SW term is comparable across the two ensembles.

The long-wave (LW) radiation budget averaged over the tropics is also summarized in Figure 3. The total GHG forcing is similar in PMIP2 and PMIP3 models. The range is slightly smaller in the former with a range of −3.0 to −2.7 W m^{-2} compared to −3.3 to −2.8 W m^{-2} in PMIP3. The clear-sky TOA minus surface LW flux corrected for this forcing is shown in Figure 3 and demonstrates a similar range in the two ensembles. Finally, the LW cloud feedbacks are distributed more widely in the PMIP3 lgm ensemble (range: −0.1 to 2.5 W m^{-2}) than in PMIP2 (range: 0.6 to 1.3 W m^{-2}).

3.1. MIROC-ESM

MIROC-ESM is the only model with a significant change in the aerosol loading. This stems from the inclusion of interactive mineral dust emissions and interactive vegetation. The dust emissions and their radiative effects are modeled using the SPRINTARS model which has been used previously for the LGM [*Takemura et al.*, 2009]. The results from *Takemura et al.* [2009] can therefore help in the interpretation of processes operating in MIROC-ESM. The total column dust loading is also similar in the simulations of *Takemura et al.* [2009] and MIROC-ESM, with preindustrial burdens of 14 and 12 Tg, respectively, and LGM burdens of 31 and 34 Tg, respectively.

In MIROC-ESM the aerosol optical depth (AOD) at 550 μm shows much larger overall changes than in the abrupt4×CO_2 simulation (not shown), and this is confirmed by the SW clear-sky feedback term, which is −1.2 W m^{-2}. MIROC-ESM also includes dynamic vegetation which makes a contribution over the tropics. Additionally, there is a substantial decrease in the albedo over the Sahara and this acts to further reduce cooling over the tropics. The SW surface albedo term is positive (0.2 W m^{-2}) in MIROC-ESM for the tropics, mostly as a result of the albedo change over the Sahara (Figure 3).

MIROC-ESM also includes the first and second indirect effects of mineral dust aerosols (see Table S1 in the supporting information). The lgm-piControl anomaly of the effective cloud top particle radius shows a significant global decrease symptomatic of the first aerosol indirect effect. Using the same aerosol model

Takemura et al. [2009] calculated a global radiative forcing due to SW indirect effects of dust at the LGM of +0.90 and +0.66 W m^{-2} at the tropopause and surface, respectively. An aerosol-induced positive SW indirect effect in MIROC-ESM could therefore account for some of the difference of the SW cloud feedback relative to the 4 × CO_2 simulation (as shown in Figure 2). The LW indirect aerosol effects simulated by *Takemura et al.* [2009] are also important but with opposing values of −1.96 W m^{-2} and +0.22 W m^{-2} at the tropopause and surface, respectively.

The analysis over the tropics shows that MIROC-ESM has the smallest SW feedback factors from any of the models analyzed, despite having the highest climate sensitivity and showing the second highest SW feedback value in the abrupt4×CO_2 experiment.

3.2. CNRM-CM5

The outstanding term in the energy balance for CNRM-CM5 is the effective greenhouse gas forcing. This term is only −8.4 W m^{-2} compared to the multimodel averages of −12.1 ± 1.8 W m^{-2} for PMIP3 and −11.6 ± 1.7 W m^{-2} for PMIP2 (clear-sky TOA surface, Figure 3). CNRM-CM3 in PMIP2 shows a similarly small value for this term (−8.9 W m^{-2}). Interestingly, the same term in the abrupt4×CO_2 simulation by CNRM-CM5 is close to the ensemble average value. This suggests that the model behaves nonlinearly in response to a cooler climate compared to a warming climate. In CNRM-CM5 compared to CNRM33 there is (i) an increase in the ECS value and (ii) a smaller LW cloud feedback term. These two terms combined induce a nearly 1 W m^{-2} difference between the two CNRM models. Unfortunately, not enough fields are stored in the PMIP2 database to perform the APRP analysis of the CNRM-CM3 PMIP2 simulation. Overall, the behavior in CNRM-CM5 is the least understood and future work is required to resolve this.

3.3. GISS-E2-R

GISS is the only model run with prescribed LGM vegetation distributions [from *Ray and Adams*, 2001]. GISS-E2-R simulates extreme cooling (−17.5°C), over middle- to high-latitude Asia (land points in the region 55–120°E by 45–75°N) possibly more as a result of the sensitivity of snow-covered vegetation albedo than because of the vegetation distribution imposed, since other PMIP3/CMIP5 models with large reductions in tree cover simulate substantially less cooling (e.g., in MPI-ESM-p cooling is −10.3°C and in MIROC-ESM it is −11.1°C) and the cooling in GISS-E2-R is substantially larger than indicated by the pollen-based temperature field reconstruction from *Bartlein et al.* [2011]. This enhanced extratropical cooling causes snow to persist north of 40–50°N throughout the year in Asia (see Figure S4) and therefore likely contributes a cooling signal at lower latitudes similar to the cooling induced by the imposition of LGM ice sheets. Thus, teleconnections, including a reduction in atmospheric water vapor act to enhance cooling in the tropics. The latter can be seen in the LW clear-sky TOA minus surface flux (Figure 3) for which GISS has the largest value of any of the LGM simulations, despite having a smaller than average value in the abrupt4×CO_2 simulation (see Table S3). GISS-E2-R also has vegetation changes in the tropics, and the surface albedo effect from these is relatively large with an average forcing of −1.4 W m^{-2} (see Figure 3). Only MRI-CGCM3 has a larger surface albedo contribution. Together, these factors help to explain the magnitude of the LGM tropical cooling in GISS-E2-R.

4. Discussion

Our analyses demonstrate that there is no coherent relationship between climate sensitivity and tropical change in CMIP5 models, and we identify several mechanisms of climate change specific to the last glacial maximum that introduce this heterogeneity. These are (i) aerosol direct and indirect effects arising from changes in aerosol loading or because of interactions between the physical climate, aerosols and clouds; (ii) surface albedo changes due to prescribed or interactively modeled vegetation changes. and (iii) changes in atmospheric emissivity due to water vapor, possibly driven by prescribed vegetation changes. Overall, we find that the CMIP5 LGM ensemble shows qualitatively different behavior from the older PMIP2 ensemble.

The correlation between ECS and tropical temperature changes is positive in both the RCP8.5 and abrupt4×CO_2 simulations (see supporting information Figure S1). The abrupt4×CO_2 output shows relatively little change in global vegetation distributions in the CMIP5 models which include dynamic vegetation, while the changes in aerosol loading are smaller than those simulated for the LGM in these models.

Together, these factors demonstrate that the PMIP3 ensemble cannot be used all together to infer climate sensitivity as was the case in PMIP2. This is because the model simulations are not drawn from an identical experimental design, but instead span a range of model component and boundary condition choices.

However, the majority of models show reasonable agreement in terms of LGM tropical cooling, with 7 and 12 of the models shown in Figure 1 lying within the upper and lower reconstruction ranges, respectively, of *Annan and Hargreaves* [2013], where the lower reconstruction is devised as a sensitivity test to account for disagreement between records derived from different proxy types of LGM sea surface temperatures [see also *Annan and Hargreaves*, 2015].

As a number of models simulate the LGM tropical temperature change reasonably well, it is not possible to say whether additional Earth System processes are required or whether the feedback strengths of these processes have been overestimated in some models. However, the extratropical model response in GISS-E2-R is markedly stronger than in the other CMIP5 models which include dynamic vegetation (MIROC-ESM and MPI-ESM-P) and GISS-E2-R significantly overestimates cooling in the Northern extratropics in comparison with the surface temperature reconstructions of *Bartlein et al.* [2011]. The model also simulates snow cover persisting into summer in this area at the LGM, indicating potential ice sheet inception, which is not supported by reconstructions. Thus, if the extratropical and tropical cooling are related in this model, then the fact that it is an outlier in terms of the ECS to tropical temperature relationship is more likely a result of oversensitivity of the model to cold conditions, as opposed to a manifestation of uncertainty in the ECS to tropical behavior for the LGM.

If the next multimodel ensemble of LGM simulations consistently included similar Earth System components, would we revive a clear ΔT_{trop} to ECS relationship? It is possible, and in this case the inferred distribution of ECS may shift to different values than inferred with PMIP2 models. There is also the possibility that the range of responses could diversify, as differences in the physical climates between models feed through into the other Earth System components like vegetation and dust. This would then imply that the relationship found in PMIP2 models is due to under-sampling of the range of possible LGM climate states, related to the omission of dust and vegetation feedbacks in the PMIP2 experimental design. In this case, idealized paleoclimate experiments focused on the LGM [e.g., *Yoshimori et al.*, 2009; *Brady et al.*, 2013] could help in distinguishing between models with different feedback strengths [e.g., *Hopcroft and Valdes*, 2014] by evaluation with paleo-environmental reconstructions.

5. Conclusions

Hargreaves et al. [2012] found a statistically significant relationship between tropical cooling and equilibrium climate sensitivity in PMIP2 coupled GCM simulations of the LGM. Here we analyze the tropical climate changes in CMIP5/PMIP3 last glacial maximum simulations and show that this relationship does not hold in this newer multimodel ensemble. Although there is some evidence that model performance plays a role in this decoupling, the inclusion of Earth System components, such as dynamic vegetation and interactive aerosols in some models is also important. Careful evaluation of the relative strengths of these additional feedbacks is required; otherwise, simulated climate anomalies could even be right for the wrong reasons, potentially leading to erroneous inferences about climate sensitivity in this context. Until a larger ensemble of models including Earth System components are available, we cannot say whether there is a useable relationship between tropical cooling and climate sensitivity which can be exploited to infer climate sensitivity from reconstructions of LGM tropical temperature anomalies.

Acknowledgments

P.O.H. was funded by the NERC grants NE/I010912/1 (Earth System Modelling of Abrupt Climate Change) and partly by NE/J005274/1 (Terrestrial Carbon Cycle Dynamics in CMIP5 Last Glacial Maximum and mid-Holocene climate simulations). We acknowledge the World Climate Research Programme's Working Group on Coupled Modelling, which is responsible for CMIP, and the climate modeling groups for producing and making available their model output. For CMIP the U.S. Department of Energy's Program for Climate Model Diagnosis and Intercomparison provided coordinating support and led development of software infrastructure in partnership with the Global Organization for Earth System Science Portals. We thank the PMIP2 modeling groups for making their model output available through the PMIP database. Thanks also to Uwe Mikolajewicz for supplying the correct orography files for MPI-ESM.

The Editor thanks two anonymous reviewers for their assistance in evaluating this paper.

References

Annan, J., and J. Hargreaves (2013), A new global reconstruction of temperature changes at the Last Glacial Maximum, *Clim. Past*, *9*, 367–376, doi:10.5194/cp-9-367-2013.

Annan, J., and J. Hargreaves (2015), A perspective on model-data surface temperature comparison at the Last Glacial Maximum, *Quat. Sci. Rev.*, *107*, 1–10, doi:10.1016/j.quascirev.2014.09.019.

Bartlein, P. J., et al. (2011), Pollen-based continental climate reconstructions at 6 and 21 ka: A global synthesis, *Clim. Dyn.*, *37*(3–4), 775–802, doi:10.1007/s00382-010-0904-1.

Berger, A., and M. Loutre (1991), Insolation values for the climate of the last 10 million years, *Quat. Sci. Rev.*, *10*(4), 297–317.

Braconnot, P., S. Harrison, M. Kageyama, P. Bartlein, V. Masson-Delmotte, A. Abe-Ouchi, B. Otto-Bliesner, and Y. Zhao (2012), Evaluation of climate models using palaeoclimatic data, *Nat. Clim. Change*, *2*, 417–424, doi:10.1038/nclimate1456.

Brady, E., B. Otto-Bliesner, J. Kay, and N. Rosenbloom (2013), Sensitivity to glacial forcing in the CCSM4, *J. Clim.*, *26*, 1901–1925, doi:10.1175/JCLI-D-11-00416.1.

Crucifix, M. (2006), Does the last glacial maximum constrain climate sensitivity?, *Geophys. Res. Lett.*, *33*, L18701, doi:10.1029/2006GL02137.

Dufresne, J., and S. Bony (2008), An assessment of the primary sources of spread of global warming estimates from coupled atmosphere-ocean models, *J. Clim.*, *21*, 5135–5144.

Forster, P., and K. Taylor (2006), Climate forcings and climate sensitivities diagnosed from coupled climate model integrations, *J. Clim.*, *19*, 6181–6194.

Gregory, J., W. Ingram, M. Palmer, G. Jones, P. Stott, R. Thorpe, J. Lowe, T. Johnes, and K. Williams (2004), A new method for diagnosing radiative forcing and climate sensitivity, *Geophys. Res. Lett.*, *31*, L03205, doi:10.1029/2003GL018747.

Hargreaves, J., J. Annan, M. Yoshimori, and A. Abe-Ouchi (2012), Can the Last Glacial Maximum constrain climate sensitivity?, *Geophys. Res. Lett.*, *39*, L24702, doi:10.1029/2012GL053872.

Harrison, S., et al. (2013), Climate model benchmarking with glacial and mid-Holocene climates, *Clim. Dyn.*, *43*(3–4), 671–688, doi:10.1007/s00382-013-1922-6.

Hopcroft, P., and P. Valdes (2014), Last Glacial Maximum constraints on the Earth System model HadGEM2-ES, *Clim. Dyn.*, doi:10.1007/s00382-014-2421-0, in press.

Kohfeld, K., and S. Harrison (2001), DIRTMAP: The geological record of dust, *Earth Sci. Rev.*, *54*, 81–114.

MARGO Project Members (2009), Constraints on the magnitude and patterns of ocean cooling at the Last Glacial Maximum, *Nat. Geosci.*, *2*, 127–132, doi:10.1038/NGEO411.

Mix, A., E. Bard, and R. Schneider (2001), Environmental processes of the ice age: Land, oceans, glaciers (EPILOG), *Quat. Sci. Rev.*, *20*, 627–657.

Peltier, W. (2004), Global glacial isostasy and the surface of the ice age Earth: The ICE-5G (VM2) model and GRACE, *Annu. Rev. Earth Planet. Sci.*, *32*, 111–149.

Petit, J., et al. (1999), Climate and atmospheric history of the past 420,000 years from the Vostok Ice Core, Antarctica, *Nature*, *399*, 429–436.

Prentice, I., D. Jolly, and BIOME 6000 participants (2000), Mid-Holocene and glacial-maximum vegetation geography of the northern continents and Africa, *J. Biogeogr.*, *27*, 507–519.

Ray, N., and J. Adams (2001), A GIS-based vegetation map of the world at the Last Glacial Maximum (25,000-15,000 BP), *Internet Archaeol.*, *11*, 1–44.

Schmidt, G., et al. (2014), Using palaeo-climate comparisons to constrain future projections in CMIP5, *Clim. Past*, *10*, 221–250, doi:10.5194/cp-10-221-2014.

Spahni, R., et al. (2005), Atmospheric methane and nitrous oxide of the late pleistocene from Antarctic ice cores, *Science*, *310*, 1317–1321.

Takemura, T., et al. (2009), A simulation of the global distribution and radiative forcing of soil dust aerosols at the last glacial maximum, *Atmos. Chem. Phys.*, *9*(20), 3061–3073.

Taylor, K., M. Crucifix, P. Braconnot, C. Hewitt, C. Doutriaux, A. Broccoli, J. Mitchell, and M. Webb (2007), Estimating shortwave radiative forcing and response in climate models, *J. Clim.*, *20*, 2530–2543.

Yoshimori, M., T. Yokohata, and A. Abe-Ouchi (2009), A comparison of climate feedback strength between CO_2 doubling and LGM experiments, *J. Clim.*, *22*, 3374–3395.